Biol. **10**, 6417 (1990); P. Legrain and A. Choulika, *EMBO J.* **9**, 2775 (1990).
16. S. Behrens, F. Gallisson, P. Legrain, R. Luhrmann, *Proc. Natl. Acad. Sci. U.S.A.*, in press.
17. K. Schappert and J. D. Friesen, *Mol. Gen. Genet.* **226**, 277 (1991).
18. M. Bennett and R. Reed, unpublished data.
19. S.-E. Behrens, K. Tyc, B. Kastner, J. Reichelt, R. Luhrmann, *Mol. Cell. Biol.* **13**, 307 (1993).
20. R. Luhrmann, B. Kastner, M. Bach, *Biochim. Biophys. Acta* **1087**, 265 (1990).
21. S. Ruby, T.-H. Chang, J. Abelson, *Genes Dev.*, in press.
22. R. Reed, unpublished data.
23. M. Bennett, R. Brosi, A. Krämer, R. Reed, unpublished data.
24. R. Brosi, H. P. Hauri, A. Krämer, *J. Biol. Chem.*, in press.
25. R. Brosi, K. Groning, S.-E. Behrens, R. Luhrmann, A. Krämer, *Science* **262**, 102 (1993).
26. P. Legrain and C. Chapon, *ibid.*, p. 108.
27. C. Chapon and P. Legrain, *EMBO J.* **11**, 3279 (1992); S. Wells and M. Ares, personal communication.
28. J. Arenas and J. Abelson, *Proc. Natl. Acad. Sci. U.S.A.* **90**, 6771 (1993); S. Ruby, personal communication.
29. D. S. McPheeters and J. Abelson, *Cell* **71**, 819 (1992); H. D. Madhani and C. Guthrie, *ibid.*, p. 803; R. Parker, P. G. Siliciano, C. Guthrie, *ibid.* **49**, 229 (1987); Y. Zhuang and A. M. Weiner, *Genes Dev.* **3**, 1545 (1989); J. A. Wu and J. L. Manley, *ibid.*, p. 1553.
30. J. Sambrook, E. Fritsch, T. Maniatis, *Molecular Cloning: A Laboratory Manual* (Cold Spring Harbor Laboratory Press, Cold Spring Harbor, NY, ed. 2, 1989).
31. P. Champion-Arnaud, D. Staknis, R. Reed, unpublished data.
32. M. Zhang, P. D. Zamore, M. Carmo-Fonesca, A. I. Lamond, M. R. Green, *Proc. Natl. Acad. Sci. U.S.A.* **89**, 8769 (1992).
33. We acknowledge the technical assistance of R. Feld and B. McCabe. We thank F. Galisson and P. Legrain for the gift of PRP9 antibodies; T.-H. Chang and J. Abelson for PRP11 antibodies; T. Celeste for cDNA libraries and useful discussions; M. Botfield for assistance with the PRP11/SAP62 protein alignment; and B. Burke for advice on Western blots. We are grateful to J. Abelson, J. Arenas, M. Ares, A. Krämer, P. Legrain, R. Luhrmann, and S. Ruby for useful discussions and communication of results before publication. R.R. is a Lucille P. Markey Scholar. Supported by a grant from the Lucille P. Markey Charitable Trust and a grant from NIH (#GM43375).

14 July 1993; accepted 3 August 1993

Interaction Between PRP11 and SPP91 Yeast Splicing Factors and Characterization of a PRP9-PRP11-SPP91 Complex

Pierre Legrain* and Christine Chapon

Several proteins are involved in the early steps of the spliceosome assembly pathway. Protein-protein interactions have been identified between two *Saccharomyces cerevisiae* yeast splicing factors, PRP9 and SPP91. Here it is demonstrated that protein-protein interactions occur between SPP91 and PRP11. The combination of the *prp9-1* mutant and a truncated *prp11* mutant exhibits a synthetic lethal phenotype, suggestive of a common biochemical defect. The PRP9 and PRP11 proteins do not interact directly, but the PRP9 and PRP11 molecules can simultaneously bind SPP91 to form a three-molecule complex. Structurally and functionally related proteins are found in mammalian cells and are associated in a single biochemical fraction. This strongly suggests that the PRP9-SPP91-PRP11 complex is a key element of the splicing machinery.

Nuclear pre-mRNA splicing occurs in a complex called the spliceosome that contains U1, U2, and U4/U6.U5 small nuclear ribonucleoprotein particles (snRNPs) bound to the pre-mRNA (*1–3*). In yeast, more than 30 factors encoded by the *PRP* genes are implicated in splicing. The recognition of intron boundaries is a critical step in splicing and involves the U1 and U2 particles and additional protein factors. During spliceosome assembly, the U2 snRNP binds to the U1 snRNP–pre-mRNA complex to form the prespliceosome. Both the PRP11 and PRP9 yeast proteins are required for prespliceosome formation. Moreover, the PRP9 protein associates with the U2 snRNP particle in a salt-dependent fashion (*4–6*).

We identified an essential gene, *SPP91*, as a second-site suppressor of the *prp9-1* mutation (*7*). The *SPP91* gene is identical to the *PRP21* gene whose product is also required for the formation of the prespliceosome (*8*). In the absence of splicing complexes, neither the PRP9 protein nor the SPP91 protein is tightly associated with the U1 or the U2 snRNPs. In contrast, when splicing reactions are performed in vitro, both PRP9 and SPP91 are found associated with the prespliceosome (*6, 8*). These observations suggest that the PRP9 and SPP91 proteins act together to promote the interaction between the U2 snRNP particle and the U1 snRNP–pre-mRNA complex. Although it is likely that protein-protein interactions play a crucial role in spliceosome assembly, very little is known about these interactions. We have demonstrated that the PRP9 and SPP91 proteins interact (*9*). Here, we demonstrate that PRP11 also binds to SPP91, and we present genetic evidence that PRP9 and PRP11 are functionally related. Moreover, with a three-molecule binding assay, we identify a multimolecular complex formed by SPP91, PRP9, and PRP11.

The PRP9 and PRP11 proteins contain cysteine-histidine motifs (CH) that are loosely related to those found in C_2H_2 zinc finger proteins (Fig. 1) (*5*). When the *PRP11* allele deleted for the CH motif (*prp11ΔCH*) was expressed in a *prp11-1* strain, a dominant lethal phenotype was observed (Fig. 2). A *prp11* allele that contained only the region downstream of the CH motif still exhibited the dominant lethal phenotype (*10*). This dominant lethal phenotype suggests that the COOH-terminal region of PRP11 contains a binding site for a factor that is titrated by the truncated protein (*11*). Expression of *prp11ΔCH* also had a strong effect on *prp9-1* cell viability but not on the viability of wild-type isogenic cells (Fig. 2). This synthetic lethal phenotype suggests that there is a close functional relation between PRP9 and PRP11 proteins. Synergistic effects have been observed between the *prp5*, *prp9*, *prp11*, and *prp21* temperature-sensitive (ts) mutations (*12*).

The possible interactions between the PRP9 and PRP11 proteins were tested with the two-hybrid system which scores for in vivo interactions between two proteins overproduced in yeast (*13, 14*). In this assay, two proteins are fused to the DNA binding domain and to the activation domain of the yeast transcriptional factor GAL4, respectively. An interaction between these proteins brings together the two GAL4 domains, allowing the formation of a functional GAL4 complex that activates the expression of a *lacZ* reporter gene. When the *PRP9* coding region was fused to the GAL4 activation domain and the *PRP11* coding region was fused to the GAL4 DNA binding domain, very low amounts of β-galactosidase activity were detected. Similar results were observed for the reciprocal combination (Fig. 3A), suggesting that PRP9 and PRP11 proteins do not interact. In contrast, in an assay with the PRP11 and SPP91 GAL4 fusion proteins, high quantities of β-galactosidase activity were detected, revealing a strong interaction between these two proteins (Fig. 3A).

This interaction was characterized in greater detail with the PRP11-1 (*15*) and PRP11ΔCH mutant proteins (Fig. 1). We assayed the interaction of the PRP11-1 protein fused to either the GAL4 activation

Unité de Génétique Moléculaire des Levures, Département de Biologie Moléculaire, Institut Pasteur, Paris 75724, France.

*To whom correspondence should be addressed.

or DNA binding domain with the reciprocal SPP91 fusion protein. In both assays we detected approximately background amounts of β-galactosidase activity. This suggests that the heat-sensitive phenotype of the *prp11-1* mutation results, at least in part, from a reduced interaction between PRP11 and the SPP91 protein (Fig. 3A). In contrast, PRP11ΔCH protein fusions exhibited a high β-galactosidase activity in either combination, similar to those obtained with the wild-type PRP11 protein, indicating that the CH motif is not involved in the binding to the SPP91 protein. These results are very similar to those obtained for PRP9. The *prp9ΔCH2* mutant exhibited a dominant lethal phenotype when expressed in *prp9-1* cells, and the PRP9 protein interacted with

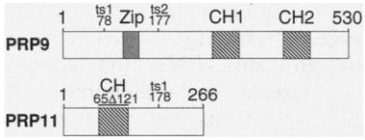

Fig. 1. The PRP9 and PRP11 proteins. Sequences of the proteins have been described (*4, 5*). The ts mutations, a putative leucine zipper (Zip, shaded box), the motifs related to the C_2H_2 zinc fingers (CH, striped boxes), and the deleted region (Δ) in the *prp11ΔCH* mutant are indicated. The mutations ts1 and ts2 in PRP9 and ts1 in PRP11 refer to the *prp9-1*, *prp9-2*, and *prp11-1* mutations, respectively (*9, 15*).

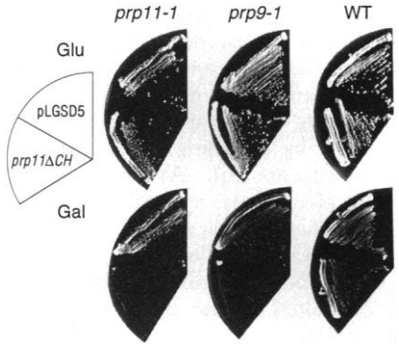

Fig. 2. The *prp11ΔCH* mutant exhibits a dominant lethal phenotype. The *prp11-1* [A635 (*25*)], *prp9-1* [Cy105 (*7*)], or isogenic wild-type [MGD353-46D (*7*)] cells were transformed with the *prp11ΔCH* or the pLGSD5 plasmid (*27*). The *prp11ΔCH* plasmid was derived from the pLGSD5 vector and harbors a *prp11ΔCH* gene whose expression is promoted from a galactose-inducible promoter. Transformants were streaked on glucose (Glu)– or galactose (Gal)–containing medium and grown at 25°C. The *prp11ΔCH* mutant was derived by site-directed mutagenesis of the wild-type gene. Two Xho I sites were introduced at positions corresponding to residues indicated (Fig. 1) and subsequently digested and religated. The gene was amplified by PCR with two flanking Bam HI sites and cloned in the pLGSD5 vector.

the SPP91 protein through a region identified by two ts mutations that is distinct from any of the PRP9 CH motifs (*9*) (Fig. 3A).

To determine whether interactions of the SPP91 protein with the PRP9 and PRP11 proteins were exclusive, we asked whether overexpression of the SPP91 protein could bridge the PRP9 and PRP11 proteins when they were fused to the GAL4 DNA binding or activation domain. The coincident binding of PRP9 and PRP11 proteins to the SPP91 protein, if it occurs, may allow the formation of a three-protein complex and result in high amounts of β-galactosidase activity. Overproduction of the SPP91 protein resulted in a 20-fold increase in β-galactosidase activity compared with cells that contained the wild-type concentration of the SPP91 protein (Fig. 3B).

We verified the specificity of this assay by performing similar experiments with several mutant combinations. The PRP11-1 protein, which interacts very poorly with the SPP91 protein, exhibited low β-galactosidase activity in this three-protein binding assay. In contrast, two mutants in the CH motifs of PRP11 or PRP9 proteins, the PRP11ΔCH and the PRP9-C423 mutant proteins (*16*), exhibited a 25- to 30-fold increase of β-galactosidase activity when tested in the three-molecule binding assay. These mutant proteins retain their ability to bind SPP91 when tested in the two-hybrid system (Fig. 3A) (*9*). Altogether, these results suggest that the PRP9, PRP11, and SPP91 proteins can form a multimolecular complex. We cannot exclude the possibility that independent PRP9-SPP91 and PRP11-SPP91 interactions promote conformational changes favoring a direct PRP9-PRP11 interaction. However, this latter hypothesis seems unlikely because PRP9ΔCH2 and PRP11ΔCH mutant proteins exhibit a similar phenotype.

The ability of PRP9 and PRP11 to bind SPP91 is independent of their CH motifs. The CH motifs are involved in another function, as demonstrated by the dominant lethal phenotype observed with *prp9ΔCH2* and *prp11ΔCH* mutants (Fig. 2) (*9, 11*). These motifs are located in the COOH-terminal and the NH_2-terminal parts of PRP9 and PRP11, respectively (Fig. 1). Thus, these proteins may be formed of independent domains, in a manner similar to the U1 snRNP–specific protein, U1C, whose CH domain is involved in the binding to the U1 snRNP (*5, 17, 18*). By analogy, the CH domains of the PRP9 and PRP11 proteins are likely candidates for regions required for binding to the snRNP particles.

Homologs of PRP9 and PRP11 have been identified in mammalian cells. A PRP9 antiserum detects one of the proteins of the 17S U2 snRNP (*19, 20*), which is also present in the splicing factor SF3a (*21, 22*). SF3a is a biochemical fraction consisting of three polypeptides (60, 66, and 120 kD) (*23*). These polypeptides are found among the spliceosome-associated proteins (SAPs) (identified as SAP 61, SAP 62, and SAP 114, respectively). Complementary DNA of SAP 62 has been cloned and is homologous to the *PRP11* gene (*24*). The

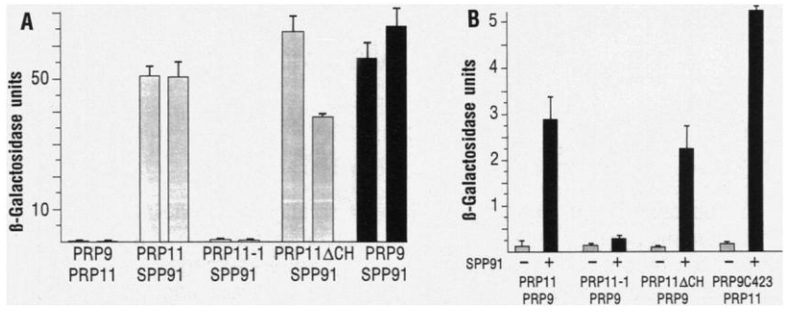

Fig. 3. Interaction between PRP9, PRP11, and SPP91 proteins. The two-hybrid system (*13, 14*) was used to monitor protein-protein interactions with proteins fused to the GAL4 DNA binding domain (GAL4 1–147) or the activation domain (GAL4 768–881) (*28*). (**A**) Direct interactions between proteins. Reciprocal combinations are presented. Interactions between PRP9 and PRP11 proteins, the SPP91 protein, and wild-type or mutant PRP11 proteins (gray bars) and between PRP9 and SPP91 proteins (black bars) are presented. The characteristics of the latter interaction were described elsewhere (*9*). (**B**) Assay for indirect binding between PRP9 and PRP11 proteins. Cells were transformed with one plasmid expressing fusion proteins with the GAL4 activation domain [PRP11, PRP11-1, PRP11ΔCH, or PRP9-C423 (*16*)] simultaneously with another plasmid expressing fusion proteins with the GAL4 DNA binding domain (PRP9 or PRP11). The *SPP91-1* gene was introduced with its own promoter in the PRP9-GAL4(1–147) or in the PRP11-GAL4(1–147) plasmid. The cells did (+, black bars) or did not (–, gray bars) overproduce the SPP91 protein. The GAL4 fusion proteins were overproduced at a very high amount compared with the endogenous expression or the plasmid-derived *SPP91* expression because the chimeric genes were under a strong promoter. Cells were grown at 30°C and β-galactosidase activity was measured at 30°C, as described (*9*), in duplicate for at least three independent transformants.

interactions between the PRP9, PRP11, and SPP91 proteins we have characterized here suggest the existence of a highly conserved multimolecular complex that is required for prespliceosome assembly. The third component of the SF3a factor, the 120-kD polypeptide, is a likely candidate for the SPP91 mammalian homolog. Thus the PRP9-PRP11-SPP91 complex may serve as a bridge between the U1 and U2 snRNPs to form the prespliceosome and to commit pre-mRNAs to the splicing pathway (*25*). The binding sites of this complex to the pre-mRNA or to the U1 and U2 snRNPs, or both, remain to be identified.

REFERENCES AND NOTES

1. M. R. Green, *Annu. Rev. Cell Biol.* **7**, 559 (1991).
2. M. J. Moore, C. C. Query, P. A. Sharp, in *The RNA World*, R. Gesteland and J. Atkins, Eds. (Cold Spring Harbor Press, Cold Spring Harbor, NY, 1993), vol. 24.
3. B. C. Rymond and M. Rosbash, in *The Molecular and Cellular Biology of the Yeast* Saccharomyces (Cold Spring Harbor Laboratory Press, Cold Spring Harbor, NY, 1992), pp. 143–192.
4. T. H. Chang, M. W. Clark, A. J. Lustig, M. E. Cusick, J. Abelson, *Mol. Cell. Biol.* **8**, 2379 (1988).
5. P. Legrain and A. Choulika, *EMBO J.* **9**, 2775 (1990).
6. N. Abovich, P. Legrain, M. Rosbash, *Mol. Cell. Biol.* **10**, 6417 (1990).
7. C. Chapon and P. Legrain, *EMBO J.* **11**, 3279 (1992).
8. J. Arenas and J. Abelson, *Proc. Natl. Acad. Sci. U.S.A.* **90**, 6771 (1993).
9. P. Legrain, C. Chapon, F. Galisson, *Genes Dev.* **7**, 1390 (1993).
10. P. Legrain and C. Chapon, unpublished results.
11. I. Herskowitz, *Nature* **329**, 219 (1987).
12. S. Ruby and J. Abelson, personal communication.
13. C. T. Chien, P. L. Bartel, R. Sternglanz, S. Fields, *Proc. Natl. Acad. Sci. U.S.A.* **88**, 9578 (1991).
14. S. Fields and O. K. Song, *Nature* **340**, 245 (1989).
15. K. Schappert and J. D. Friesen, *Mol. Gen. Genet.* **226**, 277 (1991).
16. The *prp9-C423* mutation is a substitution of the Cys^{423} residue located in the PRP9 CH2 motif (*5*). This mutation affects the homodimerization of the PRP9 protein but does not interfere with the binding to SPP91 (*9*).
17. P. T. Sillekens, R. P. Beijer, W. J. Habets, W. van Venrooij, *Nucleic Acids Res.* **16**, 8307 (1988).
18. R. L. Nelissen *et al.*, *ibid.* **19**, 449 (1991).
19. S. E. Behrens, K. Tyc, B. Kastner, J. Reichelt, R. Lührmann, *Mol. Cell. Biol.* **13**, 307 (1993).
20. S. Behrens, F. Galisson, P. Legrain, R. Lührmann, *Proc. Natl. Acad. Sci. U.S.A.*, in press.
21. A. Krämer and U. Utans, *EMBO J.* **10**, 1503 (1991).
22. R. Brosi, K. Gröning, S. Behrens, R. Lührmann, A. Krämer, *Science* **262**, 102 (1993).
23. R. Brosi, H. P. Hauri, A. Krämer, *J. Biol. Chem.*, in press.
24. M. Bennett and R. Reed, *Science* **262**, 105 (1993).
25. P. Legrain and M. Rosbash, *Cell* **57**, 573 (1989).
26. J. Ma and M. Ptashne, *ibid.* **51**, 113 (1987).
27. L. Guarente, R. R. Yocum, P. Gifford, *Proc. Natl. Acad. Sci. U.S.A.* **79**, 7410 (1982).
28. We inserted polymerase chain reaction (PCR)–derived DNA fragments encoding the appropriate PRP9, PRP11, or SPP91 open reading frames at the Bam HI site of the pGAD2F and pMA424 plasmids (*9, 13, 26*).

29. We are indebted to S. Fields and M. Werner for plasmids and strains used for the two-hybrid system. We thank J. Arenas, J. Abelson, R. Brosi, A. Krämer, M. Bennett, R. Reed, and S. Ruby for communicating unpublished results. We also thank G. Chanfreau, A. Jacquier, A. Krämer, A. Korman, and C. Transy for numerous discussions and for critically reading the manuscript. Finally, we acknowledge the continuous support and interest of B. Dujon in this work. This work was partly supported by the Universite Pierre et Marie Curie and the CNRS (URA 1149).

12 July 1993; accepted 9 August 1993

Ordered Restriction Maps of *Saccharomyces cerevisiae* Chromosomes Constructed by Optical Mapping

David C. Schwartz,* Xiaojun Li,† Luis I. Hernandez,† Satyadarshan P. Ramnarain, Edward J. Huff,† Yu-Ker Wang†

A light microscope–based technique for rapidly constructing ordered physical maps of chromosomes has been developed. Restriction enzyme digestion of elongated individual DNA molecules (about 0.2 to 1.0 megabases in size) was imaged by fluorescence microscopy after fixation in agarose gel. The size of the resulting individual restriction fragments was determined by relative fluorescence intensity and apparent molecular contour length. Ordered restriction maps were then created from genomic DNA without reliance on cloned or amplified sequences for hybridization or analytical gel electrophoresis. Initial application of optical mapping is described for *Saccharomyces cerevisiae* chromosomes.

Construction of physical maps for eukaryotic chromosomes is laborious and difficult, in part because many of the current procedures for mapping and sequencing DNA were originally designed to analyze genes rather than genomes (*1*). The electrophoretic methods that are widely used in mapping offer the advantage of good size resolution, even for large molecules, but require preparation of DNA in bulk amounts from sources such as genomic DNA or yeast artificial chromosomes (YACs) (*2*). In contrast, single-molecule techniques, such as fluorescence in situ hybridization (FISH), make use of only a limited number of chromosomes (*3*), but have not yet attained a sizing resolution comparable to that of pulsed electrophoresis (*4*). Ideally, one would like to be able to combine the sizing power of electrophoresis with the intrinsic ordering capability of FISH in order to construct accurate restriction maps very rapidly. The methodology described in this report, which we refer to as optical mapping, approaches this ideal by imaging stained, single, deproteinized DNA molecules during restriction enzyme digestion. This allows direct, ordered mapping of restriction sites.

In brief, a fluid flow was used to stretch out DNA molecules dissolved in molten agarose and fix them in place during gelation (*4*). The gelation process restrains elongated molecules from relaxing to a random coil conformation during enzymatic cleavage. A restriction enzyme is added to the molten agarose–DNA mixture, and cutting is triggered by the diffusion of Mg^{2+} into the gelled mixture, which has been mounted on a microscope slide. Fluorescence microscopy coupled with digital image processing techniques were used to record, at regular intervals, cleavage sites, which are visualized by the appearance of growing gaps in imaged molecules (*5*) and bright, condensed pools or "balls" of DNA on the fragment ends flanking the cut site. These balls form shortly after cleavage as a result of coil relaxation at the new ends. The size of the resulting fragments was determined in two ways: by measurement of the relative fluorescence intensities of the products and by measurement of the relative apparent DNA molecular lengths in the fixating gel. Maps are subsequently assembled by recording the order of the sized fragments (*6*). Averaging a small number of molecules rather than using only one improves accuracy and permits rejection of unwanted molecules (*7*).

Large DNA molecules can be stretched out in molten agarose by flow forces and then rapidly fixed in place by agarose gelation, without application of electrical fields (*4*). Experimentally, the kinetics of gelation are controlled by temperature and optimization of the annealing conditions. For our analysis, DNA coils must be critically stretched: too much and the molecule becomes difficult to image, too little and there is insufficient tension to reveal cut sites. Excessively stretched molecules present too little fluorochrome per imaging pixel, so that measured molecular intensities approach background values. Additionally,

W. M. Keck Laboratory for Biomolecular Imaging, Department of Chemistry, New York University, New York, NY 10003.

*To whom correspondence should be addressed.
†These authors contributed equally to this work.